EurJIC
European Journal of Inorganic Chemistry

Full Paper
doi.org/10.1002/ejic.202000770

Metallacoronates

Structural Diversity of Alkaline Earth Centered Gold(I) Metallacoronates

Suelen Ferreira Sucena,[a][‡] Thu Thuy Pham,[b] Adelheid Hagenbach,[a] Chien Thang Pham,*[b] and Ulrich Abram*[a]

Abstract: One-pot reactions of the catechol-scaffolding aroylbis(*N*,*N*-diethylthiourea) H_2L^{cat} with mixtures of alkaline earth nitrates $M(NO_3)_2$ (M^{2+} = Ca^{2+}, Sr^{2+} or Ba^{2+}) and $(NEt_4)[AuCl_4]$ or [Au(tht)Cl] (tht = tetrahydrothiophene) in methanol in the presence of Et_3N as supporting base give rise to neutral trinuclear gold(I) {2}-metallacoronates with the composition of {M ⊂ $[Au_2(L^{cat})_2]$} (**1**). Similar reactions with the pyridine-centered aroylbis(*N*,*N*-diethylthiourea) H_2L^{py}, however, produce complexes with the same metal-to-ligand ratio but with higher nuclearity {2M ⊂ $[Au_4(L^{py})_4]$} (**2**). In both **1** and **2**, Au(I) ions are exclusively *S*-bonded with the organic ligands and adopt a virtually linear coordination fashion. Such metal-ligand binding is responsible for the formation of metallacoronands, which accommodate alkaline earth metal ions in their molecular voids, thereby resulting in host–guest coordination assemblies. The level of metal-ligand aggregation in the resulting assemblies is dependent on the denticity, size and flexibility of the centered building block of the aroylbis(*N*,*N*-diethylthiourea) ligands.

Introduction

The coordination chemistry of aroyl-*N*,*N*-dialkylthioureas is pioneered by the work of L. Beyer et al.[1] and attracted the interests of many other chemists during the last four decades. Most contributions in this field focus on the aroyl mono-HL^{ben} and bis-thioureas H_2L^{pth} (Scheme 1), which are versatile chelators for most transition metal ions.[2–11] The structural chemistry of metal complexes with aroyl-*N*,*N*-dialkylthioureas is dominated by the monoanionic *S*,*O*-chelating fashion of aroylthiourea moieties (see Scheme 1). It is interesting that with the two *S*,*O*-chelating moieties in the symmetrical bipodal phthaloylbis(*N*,*N*-dialkylthioureas) m-/p-H_2L^{pth} and divalent metal ions such as Ni^{2+}, Pt^{2+} or Cu^{2+}, which prefer square-planar or pseudoplanar coordination spheres, multinuclear complexes are formed. The structures of the resulting multinuclear systems strongly depend on the relative positions of the substituted aroylthiourea groups. In particular, para-H_2L^{pth} ligands yield trinuclear compounds $[M_3(p\text{-}L^{pth}\text{-}S,O)_3]$ (M^{2+} = Ni^{2+}, Pt^{2+}) (**I**),[4,11–13] while *meta* substitution gives rise to binuclear complexes of the general formula $[M_2(m\text{-}L^{pth}\text{-}S,O)_2]$ (M^{2+} = Co^{2+}, Ni^{2+}, Cu^{2+}, Pt^{2+}, $\{PtX_2\}^{2+}$ for X = Cl, Br or I, $\{ReO(OMe)\}^{2+}$) (**II**).[9–11,14–17] Although the obtained multinuclear complexes possess large central voids, these voids are empty and cannot accommodate any guest atoms or molecules due to the lack of donor atoms and, more seriously, the restricted effective space caused by the hydrogen atoms of the central phenyl rings pointing toward the centers.

Recently, the modification of m-H_2L^{pth} by the replacement of the phenylene ring by other spacers possessing potential donor atom(s) such as a disubstituted pyridine ring (H_2L^{py}) or a catechol building block (H_2L^{cat}) brought about a new generation of ligands with bifunctional coordination sites each of which favorably binds to a particular type of metal ions. Such interesting structural features gave access to the syntheses of a large variety of trinuclear bimetallic complexes from simple one-pot reactions of the ligands and mixtures of two metal ions with different Pearson's acidity.[18–20] In such self-assembling processes, the "soft" metal ions prefer bonding to the satellite aroylthiourea moieties, while the harder ions such as alkali, alkaline earth metal or lanthanide ions are directed to the central binding sites. As a result of this selective coordination, trinuclear, bimetallic systems could be recognized as host–guest compounds, for example the Zn(II) {2}-metallacoronate **III** or the Fe(III) {2}-metallacryptate **IV** (see Scheme 2),[19,21] where the "hard" guest ions are encapsulated in metallamacrocycles consisting of the ligands and the softer metal ions.

A number of studies show that such inclusion compounds with diverse compositions, structures and physicochemical properties can be rationally designed by self-assembly from a

[a] *Dr. S. F. Sucena, Dr. A. Hagenbach, Prof. Dr. U. Abram*
Institute of Chemistry and Biochemistry, Freie Universität Berlin, Fabeckstr. 34/36, 14195 Berlin, Germany
E-mail: ulrich.abram@fu-berlin.de
https://www.bcp.fu-berlin.de/chemie/chemie/forschung/InorgChem/agabram/index.html
[b] *T. T. Pham, Dr. C. T. Pham*
Department of Inorganic Chemistry, VNU University of Science, Vietnam National University,
Hanoi, 19 Le Thanh Tong, Hanoi, Vietnam
E-mail: phamchienthang@hus.edu.vn
https://www.chemvnu.edu.vn/
[‡] Present address: Federal Institute of Goiás, Rua 64 esq. c/ Rua 11, s/n Expansão Parque Lago, Formosa, GO 73813–816, Brazil
Supporting information and ORCID(s) from the author(s) for this article are available on the WWW under https://doi.org/10.1002/ejic.202000770.

Full Paper
doi.org/10.1002/ejic.202000770

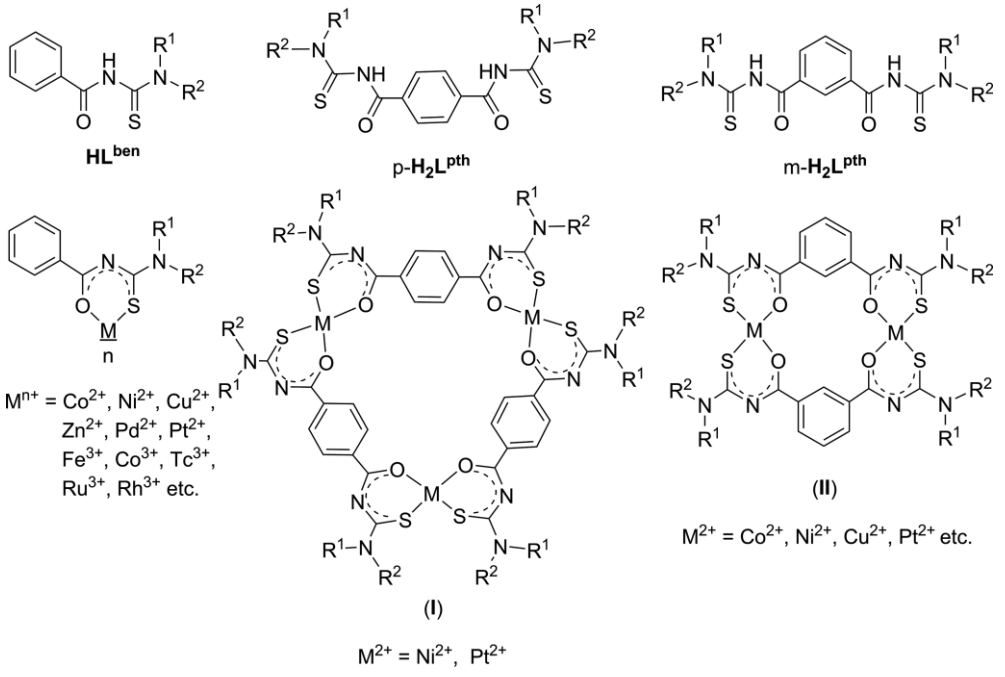

Scheme 1. Mono- and bipodal aroyl(*N*,*N*-dialkylthioureas) and their complexes.

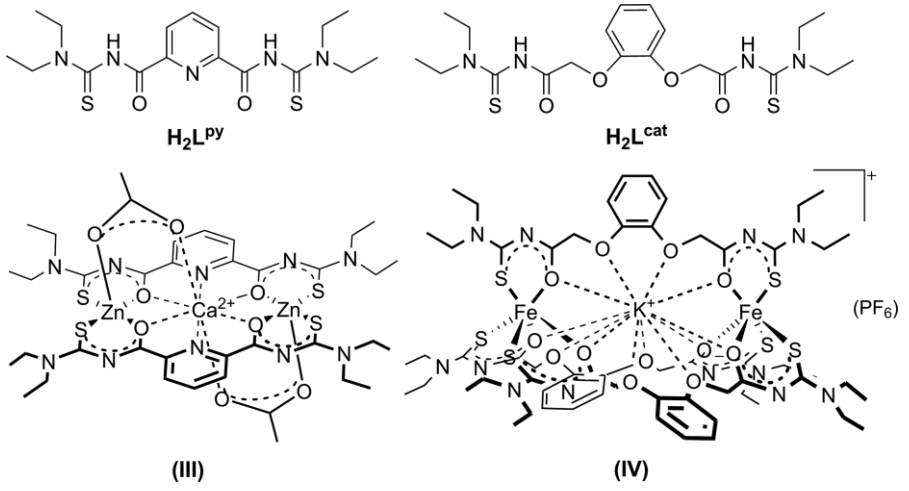

Scheme 2. Fuctionalized aroylbis(*N*,*N*-dialkylthioureas) and representatives of trinuclear bimetallic assemblies.

mixture of metal ions and the ligands H_2L^{cat} or H_2L^{py}.[18–20,22,23] To get deeper insight in the control of the self-assembling process, in this report, the utilization of the ligands H_2L^{cat} and H_2L^{py} as subunits for the construction of host–guest assemblies is continued.

Although the transition metal complexes of aroyl-*N*,*N*-dialkylthioureas have been extensively studied, surprisingly, their coordination compounds with thiophilic cations, such as Cu^+, Ag^+, Hg^{2+} and Au^+, are not well-explored. A literature survey shows only a few reports on structures of aroylthiourea complexes with Cu^+,[24–27] Ag^+,[28–32] or Hg^{2+} ions,[33–35] and only two descriptions of Au(I) complexes.[36,37] Because of the high thiophilicity of these ions, in all of their structurally characterized compounds, they are exclusively *S*-bonded to aroylthiourea ligands. This means, they essentially coordinate in the same way as unsubstituted thioureas and their derivatives.[38–47] Very recently, such flexible coordination fashion is also observed in inclusion complexes built from H_2L^{cat}, alkaline earth metal and Ag^+ or Hg^{2+} ions.[20] In this context, we extend the research to the Au(I) host–guest coordination compounds based on the versatile H_2L^{cat} and H_2L^{py} ligands.

Results and Discussion

Reactions of H_2L^{cat} (4 equiv.) with methanolic solutions containing mixtures of alkaline earth nitrates (1 equiv.) and the common Au(III) starting material $(Et_4N)[AuCl_4]$ (2 equiv.) give rise to colorless solids with the chemical composition $\{M \subset [Au_2(L^{cat})_2]\}$ (**1**) (M^{2+} = Ca^{2+} (**1a**), Sr^{2+}(**1b**) and Ba^{2+} (**1c**)). The color of the products gives a good hint for the formation of Au(I) complexes from the reduction of $(Et_4N)[AuCl_4]$ by H_2L^{cat} as reducing agent.

Full Paper
doi.org/10.1002/ejic.202000770

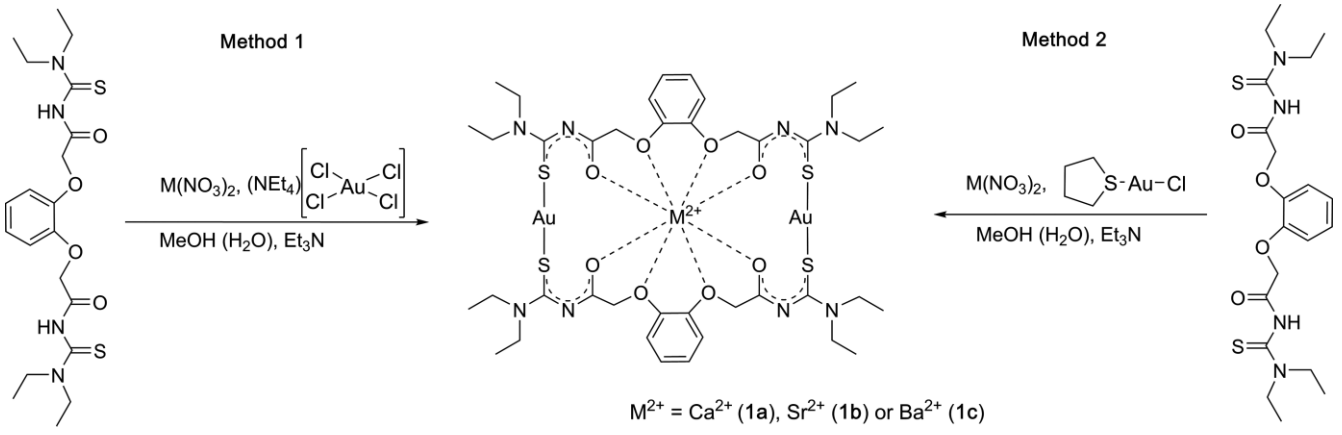

Scheme 3. Procedures for the synthesis of the {M ⊂ [Au(L^{cat}-κ*S*)]$_2$} (**1**) complexes.

This assumption is consistent with the fact that a large excess of H_2L^{cat} must be provided to get a maximum yield. Furthermore, similar redox reactions were found in the literature, when Au(III) compounds were allowed to react with *N*,*N*-dialkyl-N′-benzoylthioureas of the type HL^{ben}.[36,37,48] Identical products are obtained from an alternative approach using [Au(tht)Cl] as gold starting material with an exact stoichiometric ratio of the reactants (Scheme 3). With this second method, undesired side-reactions can be avoided and higher yields are obtained.

X-ray diffraction analyses were performed on single crystals obtained from the slow evaporation of CH_2Cl_2/MeOH, $CHCl_3$/EtOH or CH_2Cl_2/MeCN solution of **1a**, **1b**, or **1c.** The structures of **1a** and **1c** are shown in Figure 1 and selected bond lengths, bond angles and intermetallic distances are given in Table 1. Due to an unsatisfactory crystal quality of **1b**, the derived crystallographic data are not suitable to discuss in detail bond lengths and angles, but are sufficient to invoke the general structural features of the complex. Structural details of this compound are given in the Supporting Information together with its molecular structure (Figure S2.3).

Structural analyses indicate neutral trinuclear host–guest compounds with the composition {M ⊂ [Au(L^{cat})]$_2$} (M = Ca^{2+}, Sr^{2+} or Ba^{2+}). In all structures, the Au^+ ions are exclusively bonded to two soft *S* donor atoms of two deprotonated $\{L^{cat}\}^{2-}$ ligands. This behaviour is not surprising with regard to the high thiophilicity of Au(I) ions. The Au–S bond lengths vary from 2.290(3) to 2.294(2) Å and are slightly shorter than those found in a Au(I) complex with the *m*-H_2L^{pth} ligand.[37] The minor deviations of the S–Au–S bond angles (Table 1) from 180° point out the linear coordination mode of the Au centers. The linkage between two Au^+ ions and two *S*-bonded aroylthioureato ligands $\{L^{cat}\}^{2-}$ leads to a {2}-metallacoronand $[Au_2(L^{cat}\text{-}\kappa S)_2]^{2-}$ unit, which can capture guest alkaline earth metal ions M^{2+} in their central cavities by interactions with all oxygen donors of the ligand backbones. The shorter M–$O_{carbonyl}$ distances compared to M–O_{ether} ones indicate that more negative charge is located on the carbonyl O atoms than on the ether O atoms. A comparison between the structures of the three {2}-metallacoronates reveals significant differences in (i) their metal–metal distances, (ii) the coordination environment of the host ions and (iii) the conformation of the ligand skeletons. Specifically,

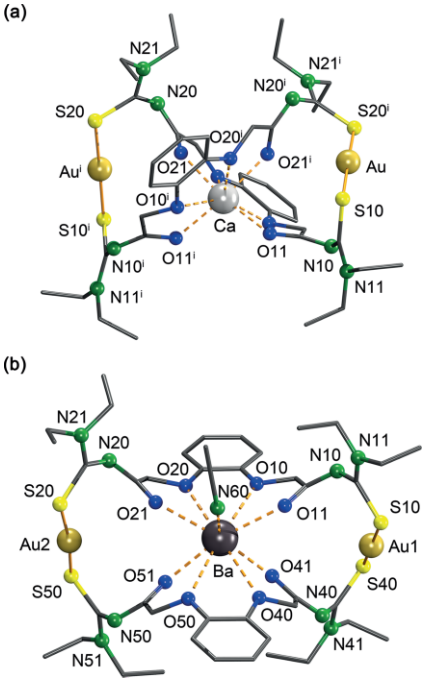

Figure 1. Molecular structures of the Au(I) {2}-metallacoronates (a) {Ca ⊂ [$Au_2(L^{cat}\text{-}\kappa S)_2$]} (**1a**) and (b) {(MeCN)Ba ⊂ [$Au_2(L^{cat}\text{-}\kappa S)_2$]} (**1c**·MeCN). Symmetry operations used to generate equivalent atoms: ^{i}–x + 1, y, –z + 3/2. Hydrogen atoms are omitted for clarity.

the smaller ions Ca^{2+} and Sr^{2+} are eight-coordinate and adopt snub-diphenoidal coordination polyhedra,[49] while one additional coordinating acetonitrile molecule is responsible for the coordination number nine of the Ba^{2+} ion with a "hulla-hop" coordination geometry (Figure 1b).[50,51] Furthermore, the deviation of the C(S)-NEt_2 moieties in opposite directions from the mean plan of the ligands causes a twisted conformation, which in turn produces the helical Ca^{2+}- or Sr^{2+}-binding complexes with dihedral angles between two mean plans of the ligands of 78.01(2)° and 76.32(2)° respectively (Figure S2.2 and S2.4). A similar deviation but in the same direction brings about the untwisted conformation, which induces a larger void, thereby resulting in a Ba^{2+} inclusion compound with a narrow dihedral

Full Paper
doi.org/10.1002/ejic.202000770

Table 1. Selected bond lengths, intermetallic distances [Å] and angles [°] in **1a** and **1c**.[a]

1a		**1c**			
Au–S10	2.2902(7)	Au1–S10	2.298(2)	Au2–S20	2.287(2)
Au–S20	2.2937(7)	Au1–S40	2.290(2)	Au2–S50	2.281(2)
Ca–O10	2.529(2)	Ba–O10	2.962(3)	Ba–O40	2.833(3)
Ca–O11	2.336(2)	Ba–O11	2.669(3)	Ba–O41	2.691(3)
Ca–O20	2.505(2)	Ba–O20	2.919(3)	Ba–O50	2.892(3)
Ca–O21	2.299(2)	Ba–O21	2.708(4)	Ba–O51	2.715(4)
Au···Au	9.5003(3)	Au1···Au2	10.8933(5)	Ba–N60	2.976(6)
Au···Ca	4.9048(1)	Au1···Ba	5.5155(3)	Au2···Ba	5.4457(2)
O11–C11	1.256(3)	O11–C11	1.246(6)	O41–C41	1.256(6)
N10–C11	1.318(3)	N10–C11	1.308(6)	N40–C41	1.317(6)
N10–C12	1.342(3)	N10–C12	1.341(6)	N40–C42	1.350(6)
N11–C12	1.330(3)	N11–C12	1.333(7)	N41–C42	1.331(7)
S10–C12	1.756(3)	S10–C12	1.742(6)	S40–C42	1.746(5)
O21–C21	1.250(3)	O21–C21	1.238(6)	O51–C51	1.233(6)
N20–C21	1.318(3)	N20–C21	1.316(6)	N50–C51	1.319(6)
N20–C22	1.361(3)	N20–C22	1.341(7)	N50–C52	1.344(7)
N21–C22	1.321(3)	N21–C22	1.335(7)	N51–C52	1.323(7)
S20–C22	1.741(3)	S20–C22	1.732(6)	S50–C52	1.747(6)
S10–Au–S20^{i}	176.47(2)	S10–Au1–S40	177.53(5)	S20–Au2–S50	173.19(6)

[a] Symmetry operations used to generate equivalent atoms: ^{i} –x + 1, y, –z + 3/2.

angle of 4.91(8)° (Figure S2.6), hence, without helicity. The partial double bond character of C–S, C–O and C–N bonds indicates the well-known π-electron delocalization in deprotonated aroylthioureas. However, this delocalization of electron density is smaller than in the previously reported compounds with chelating aroylthioureas.[19] The longer C–S and the shorter C–O bonds in the compounds of the present study indicate a higher degree of electron density on sulfur atoms of the coordinated aroylthioureas.

In addition to the X-ray structural analyses, the bonding situation of the host–guest assemblies was characterized by spectroscopic methods. In the IR spectra of the complexes, strong bands in the region between 1570 and 1590 cm^{-1} can be assigned to the $\nu_{C=O}$ stretches. This corresponds to bathochromic shifts in the range of 70 cm^{-1} to 90 cm^{-1} with regard to the uncoordinated ligand. In comparison with the common values of approximately 150 cm^{-1} for chelating aroylthioureas,[18,19,52] the shift is modest and confirms that the C-O bonds possess

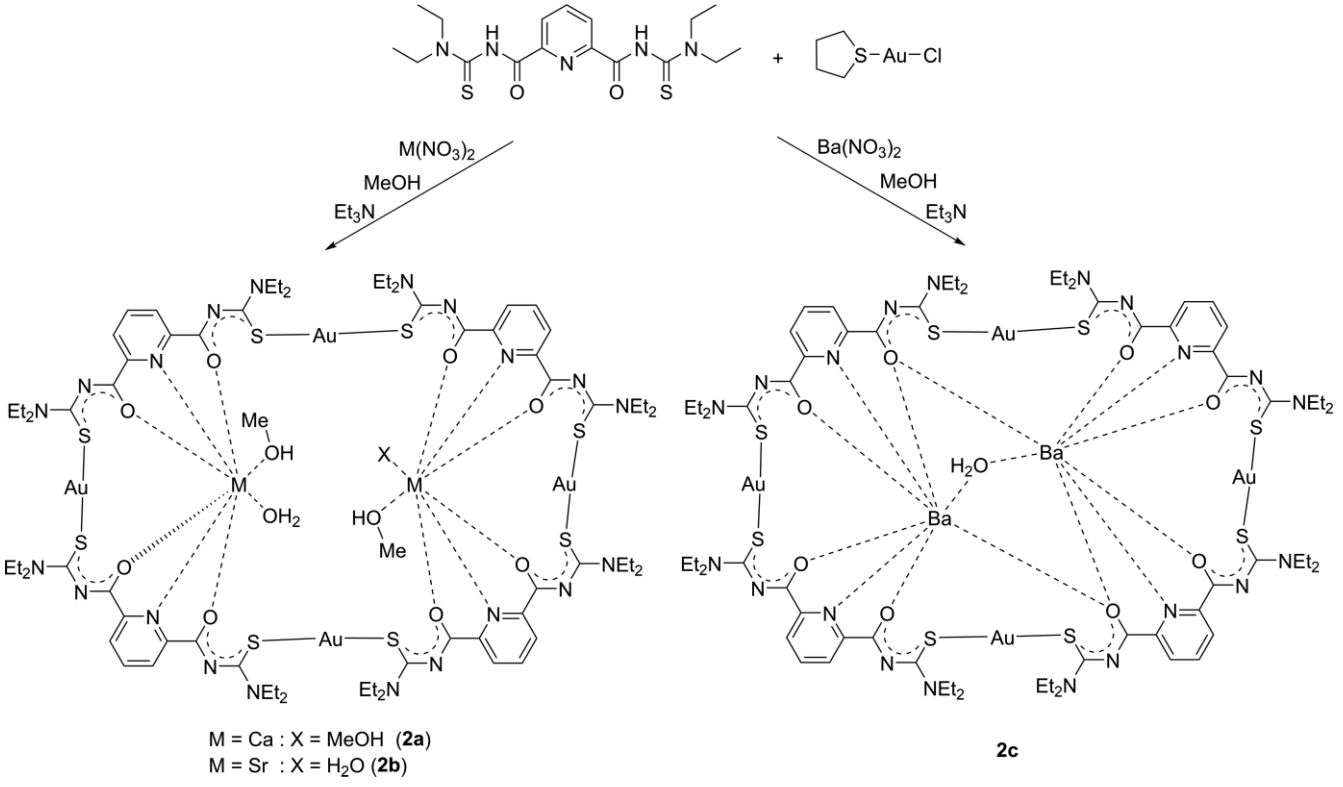

Scheme 4. Syntheses of the {2M ⊂ [$Au_4(L^{py}$-κS)$_4$]} (**2**) complexes.

Full Paper
doi.org/10.1002/ejic.202000770

more double bond character in the anionic *S*-bonded aroylthioureato ligands. The existence of the ligands in their deprotonated form $\{L^{cat}\}^{2-}$ is confirmed by the disappearance of the ν_{NH} stretches in the region above 3100 cm^{-1} in the IR spectra as well as by the absence of the signal corresponding to the NH protons in their ^1H NMR spectra. It is interesting that the splitting patterns of the methylene protons of the OCH_2 and NCH_2 groups illustrate the varying rigidity of the organic framework in the resulting complexes. In the ^1H NMR spectra of **1b** and **1c** (Figure S1.9 and S1.12), the signals assigned to OCH_2 and NCH_2 protons resemble the corresponding resonances in the ^1H NMR spectrum of the ligand. Particularly, the signal belonging to the OCH_2 protons appears as a broad singlet at about 4.9 ppm and the resonances of the NCH_2 protons are detected in the range 3.0–4.0 ppm as two broad signals or two quartets for **1b** and **1c** respectively. In contrast to the simple pattern described above, the ^1H NMR spectrum of **1a** reveals two singlets around 4.8 ppm with the typical geminal spin-spin coupling constants of 13.0–13.5 Hz for OCH_2 protons and three sextets in the range 3.2–3.7 ppm with ABX_3 splitting patterns, where J_{AB} (ca. 14.0 Hz) is approximately twice of J_{AX} (ca. 7.0 Hz), for NCH_2 protons (Figure S1.6). The more delicate fine structures of the signals associated with the methylene protons in **1a** is a strong evidence for the significant increase of the rotation barrier around the O-CH_2 and C(S)-NEt_2 bonds, in other words of the rigidity of the organic backbones, due to accommodating the smaller Ca^{2+} guest ion. Despite of the complication of the ^1H NMR spectra, the corresponding ^{13}C NMR spectra (Figure S1.7, S1.10 and S1.13) are straightforward because of an only small influence of the hindered rotation around the C(S)-NEt_2 bonds. Therefore, the resonances of the CH_2 and CH_3 carbon atoms of the NEt_2 groups appear as two separate signals in the upfield region from 10 ppm to 50 ppm. The signals belonging to the OCH_2 carbon atoms are found around 72 ppm, while those of the aromatic carbon atoms are in the range of 110 ppm to 150 ppm. The weak signals at approximately 180 ppm and 170 ppm are attributed to the resonances of C=O and C=S carbon atoms, respectively.

With the aim of constructing the similar Au(I)-metallacoronates **2** derived from the pyridine-centered ligand H_2L^{py}, the same synthetic route was applied for reactions between H_2L^{py} and mixtures of [Au(tht)Cl] and alkaline earth nitrates $M(NO_3)_2$ (M^{2+} = Ca^{2+}, Sr^{2+} or Ba^{2+}) (Scheme 4). Such reactions result in analytically pure, neutral products, which deposit from the methanolic reaction mixtures in good yields. Assuming that H_2L^{py} could perform the same coordination mode as H_2L^{cat}, the obtained products should have the compositions of $\{M \subset [Au_2(L^{py})_2]\}$, which would resemble those of the preceding compounds. The assumption was (preliminarily) supported by the elemental analyses as well as mass spectroscopic studies with the appearance of signals matching the expected fragments $\{M \subset [Au_2(L^{py})_2] + Na\}^+$ in the ESI^+ mass spectra of the complexes. However, the same mass spectra show signals with higher *m/z* values, which could be explained by a cluster ion formation in the matrix, but may also indicate that the inclusion compounds formed with the pyridine-based thiourea derivative have a higher nuclearity.

The question could be answered by the determination of the crystal structures of the compounds **2.** The structures clearly confirm the formation of larger aggregates with the general composition of $\{2M \subset [Au_4(L^{py}\text{-}\kappa S)_4]\}$. The products possess the same metal-to-ligand ratio, but a higher nuclearity than the inclusion compounds of type **1**. Figure 2 presents the structures of the Ca^{2+}- (**2a**), Sr^{2+}- (**2b**) and Ba^{2+}- (**2c**) containing complexes. Selected bonding parameters are listed in Table 2.

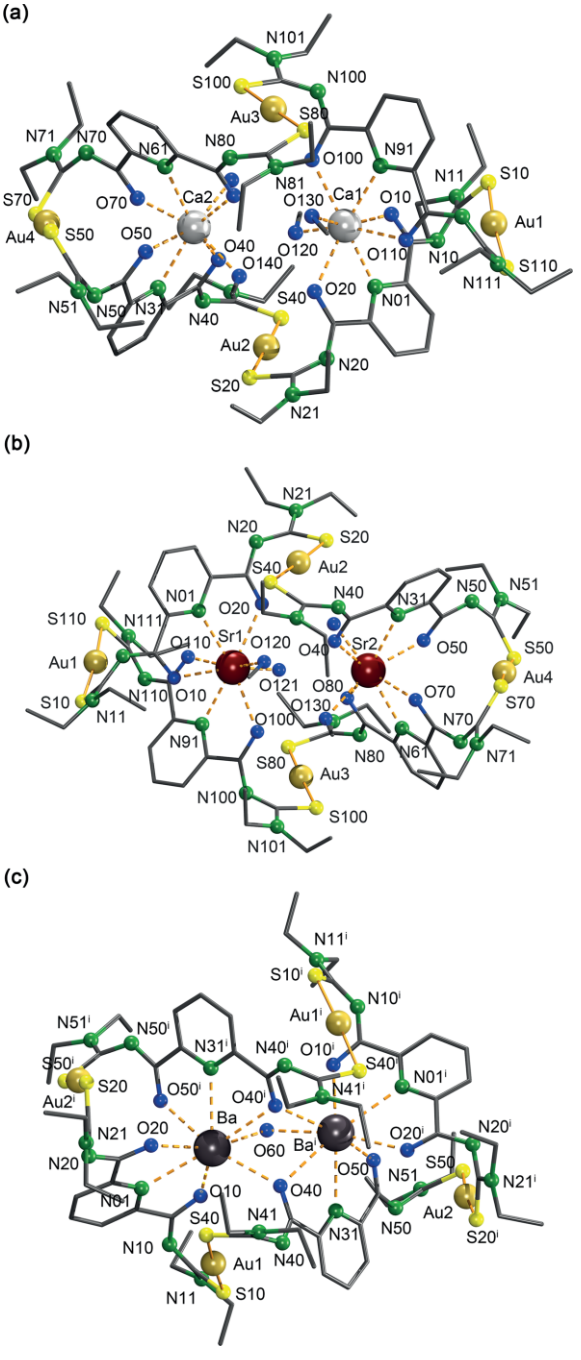

Figure 2. Molecular structures of the Au(I) {4}-metallacoronates (a) $\{(MeOH)_3(H_2O)Ca_2 \subset [Au_4(L^{py}\text{-}\kappa S)]_4\}$ (**2a**·3MeOH·H_2O), (b) $\{(MeOH)_2(H_2O)_2Sr_2 \subset [Au_4(L^{py}\text{-}\kappa S)_4]\}$ (**2b**·2MeOH·2H_2O) and (c) $\{(\mu\text{-}H_2O)Ba_2 \subset [Au_4(L^{py}\text{-}\kappa S)_4]\}$ (**2c**·H_2O). Symmetry operations used to generate equivalent atoms: ^{i} –x + 3/2, y, –z + 3/2. Hydrogen atoms are omitted for clarity.

Full Paper
doi.org/10.1002/ejic.202000770

Table 2. Selected bond lengths, intermetallic distances [Å] and angles [°] in the inclusion compounds of type **2**[a]

	2a	**2b**	**2c**	
Au1–S10/Au1–S110	2.280(2)/2.275(2)	2.270(4)/2.269(4)	Au1–S10	2.277(4)
Au2–S20/Au2–S40	2.273(2)/2.283(2)	2.302(3)/2.275(3)	Au1–S40	2.303(3)
Au3–S80/Au3–S100	2.288(2)/2.296(2)	2.278(3)/2.283(3)	Au2–S20^{i}	2.285(3)
Au4–S50/Au4–S70	2.285(2)/2.287(2)	2.279(4)/2.292(4)	Au2–S50	2.272(3)
M1···Au1/M2···Au4	5.088(2)/4.987(2)	5.161(2)/5.077(2)	Ba···Au1	4.0857(8)
M1···Au2/M2···Au2	5.082(1)/5.193(2)	5.166(2)/5.062(2)	Ba···Au2^{i}	5.3444(9)
M1···Au3/M2···Au3	5.104(2)/5.021(2)	5.084(1)/5.248(1)	Ba···Au1^{i}	6.3258(7)
M1···M2	5.118(3)	5.076(2)	Ba···Ba^{i}	4.429(1)
M1–O10/M2–O70	2.486(5)/2.435(5)	2.561(8)/2.553(9)	Ba–O10	2.782(7)
M1–O20/M2–O80	2.538(4)/ 2.586(5)	2.621(8)/ 2.651(9)	Ba–O20	2.737(7)
M1–O100/M2–O40	2.522(5)/ 2.586(5)	2.623(7)/ 2.657(8)	Ba–O40^{i}	2.854(6)
M1–O110/M2–O50	2.445(4)/ 2.413(5)	2.610(9)/ 2.564(9)	Ba–O50^{i}	2.790(7)
M1–N01/M2–N61	2.490(6)/ 2.506(7)	2.63(1)/ 2.64(1)	Ba–N01	2.918(7)
M1–N91/M2–N31	2.489(5)/ 2.490(6)	2.64(1)/ 2.65(1)	Ba–N31^{i}	2.856(9)
M1–O120/M2–O150	2.405(5)/ 2.397(5)	2.546(8)/ 2.55(1)	Ba–O40	2.777(6)
M1–O130/M2–O140	2.404(5)/ 2.391(5)	2.542(9)/ 2.542(9)	Ba–O60	2.896(7)
			Ba–S40	3.536(3)
S10–Au1–S110/S70–Au4–S50	173.26(7)/ 174.52(8)	173.1(2)/ 174.3(2)	S10–Au1–S40	177.2(1)
S20–Au2–S40/S80–Au3–S100	177.67(7)/ 178.64(7)	178.1(1)/ 177.3(1)	S20^{i}–Au2–S50	174.4(1)

[a] Symmetry operations used to generate equivalent atoms: ^{i} –x + 3/2, y, –z + 3/2.

The hexanuclear coordination assemblies $\{2M \subset [Au_4(L^{py}\text{-}\kappa S)_4]\}$ result from the encapsulation of alkaline earth metal ions M^{2+} in the void of metallacorands consisting of four Au(I) ions and four deprotonated ligands $\{L^{py}\}^{2-}$. The gold ions are exclusively bonded by the sulfur atoms of the organic ligands in a virtually linear fashion. The lower degree of π-electron delocalization in the deprotonated S-bonded aroylthiourea moieties is confirmed by the corresponding C-S, C-O and C-N bond lengths (Table S2.1 to S2.3). The pyridinedicarboxamide moieties serve as planar tridentate ligand systems and coordinate the guest M^{2+} ions through their *ONO* donor sets. Furthermore, small coordinating solvent molecules saturate the coordination spheres of such divalent ions. In the isostructural compounds **2a** and **2b**, each alkaline earth metal ion is coordinated by two pyridinedicarboxamide moieties, methanol and/or water molecules. This leads to the coordination number of eight with a biaugmented trigonal prismatic coordination geometry around the guest metal ions.[49] In contrast to the coordination environments observed in **2a** and **2b**, a coordination number of nine is found for the Ba^{2+} ions in compound **2c.** The Ba^{2+} ions adopt a "muffin-shape" coordination polyhedron by directional interactions with two pyridinedicarboxamide groups, one bridging carbonyl oxygen atom, one bridging water molecule and one sulfur atom with a Ba-S(40) distance of 3.536(3) Å.[50,51]

Spectroscopic studies on **2** are in a good agreement with the conclusion drawn from the solid-state structures. The IR spectra of the resulting {4}-metallacoronates **2** are quite similar to those of the previously discussed {2}-metallacoronates **1**. The absence of ν_{NH} bands in the region above 3100 cm^{-1} indicates the double deprotonation of H_2L^{py} during the complex formation. In addition, the modest bathochromic shifts of the $\nu_{C=O}$ bands by only approximately 85 cm^{-1} to the area around 1550 cm^{-1} proves the coordination of the oxygen atoms of the carboxamide groups with the metal ions and confirms the only moderate delocalization of π-electron density within the aroylthiourea moieties as being concluded from the crystallographic studies. The ^{1}H NMR spectra of **2** confirm the deprotonation of the ligands through the disappearance of the NH signal, which appears in the spectrum of the non-coordinated ligand around 9.0 ppm. In all spectra, the resonances in the range of 7.5–8.0 ppm are attributed to protons of disubstituted pyridine rings, while broad signals at 1.15 ppm and around 3.6 ppm are assigned to the CH_3 and CH_2 protons respectively. This NMR line broadening is a clear sign for the hindered rotation of the -NEt_2 group in the Et_2N-C(S)- fragment. Such effect is also detected in the ^{13}C NMR spectra by the splitting patterns of resonances of the carbon atoms appearing in the range of 120 ppm to 160 ppm. The weak signals at approximately 180 ppm and 170 ppm are assigned to the resonances of C=O and C=S carbon atoms, respectively. In comparison with the simple NMR pattern of **2b** and **2c**, the fine-structures of spectral lines corresponding to *ortho*-H of pyridine ring, CH_2 and CH_3 protons in the ^{1}H NMR spectrum of **2a** (Figure S1.19) as well as the two sets of signals with the 1:1 ratio in the ^{13}C NMR spectrum of **2a** (Figure S1.20) demonstrate the magnetic nonequivalence of the two halves of each $\{L^{py}\}^{2-}$ anion in solution. This phenomenon reflects a significant increase of the rigidity of the organic skeleton in **2a** due to the coordination of the guest Ca^{2+} ion. Such bonding characteristics have also been observed in **1a**. The results of the structure analysis also shed light on the ESI mass spectra of **2**. The appearance of the expected peaks ascribed to the molecular ion of the cyclic tetrameric complexes, namely $[\mathbf{2a} + Na]^+$, $[\mathbf{2b} + H]^+$ and $[\mathbf{2c} + Na]^+$, confirms their compositions. The fragments related to the "dimers" $\{M \subset [Au_2(L^{py})_2] + Na\}^+$ result from the fragmentation of the molecular ions.

A comparison of the compositions and structures of the self-assembled inclusion compounds **1** and **2** demonstrates that due to its lower denticity, size and flexibility, the ligand H_2L^{py} forms larger metallamacrocycles than the corresponding catechol-based ligand. Particularly, the higher flexibility of H_2L^{cat} due to its aliphatic backbone may enable this compound to provide the lone pairs of the donor atoms in positions for a

Full Paper
doi.org/10.1002/ejic.202000770

more efficient coordination of the large alkaline earth ions, which in return gives the cations more influence to act as templates during the self-assembly of the multi-metallic compounds. More experiments with other metal ions are in preparation to shed more light to this points.

Conclusions

Two series of Au(I) metallacoronates encapsulating alkaline earth metal ions have been prepared by one-pot reactions using catechol- and pyridine-scaffolding aroylbis(*N*,*N*-diethylthioureas). The almost linear coordination of *S*-bonded Au(I) centers with such ligands produces two types of products: (i) the {2}-metallacorands $[Au_2(L^{cat})_2]^{2-}$ and (ii) the {4}-metallacorands $[Au_4(L^{py})_4]^{4-}$. The central voids of the obtained metallacycles capture one and two alkaline earth metal ions, respectively. The denticity, size and flexibility of the central spacers exert considerable influence on the level of metal-ligand aggregation, and, thus, the compositions and structures of the resulting host–guest coordination assemblies.

Experimental Section

Materials. All chemicals used in this study were reagent grade and used without further purification. Solvents were dried and used freshly distilled unless otherwise stated. [Au(tht)Cl] was prepared by the standard procedure.[53] The ligands were synthesized according to the procedures recently reported.[19]

Physical measurements. IR spectra were measured as KBr pellets on a Shimadzu FTIR-spectrometer between 400 and 4000 cm^{-1}. ^1H and ^{13}C NMR spectra were taken with an Ascend 500 MHz multinuclear spectrometer. ESI mass spectra were measured with an Agilent 6210 ESI-TOF (Agilent Technology) mass spectrometer. All MS results are given in the form: *m*/*z*, assignment. Elemental analysis of carbon, hydrogen, nitrogen, and sulfur were determined using a Heraeus Vario EL elemental analyzer. Reproductions of the IR, NMR and MS spectra are given as Supporting Information.

Syntheses of the complexes

{M ⊂ $[Au_2(L^{cat}$-κ*S*$)_2]$} (M^{2+} = Ca^{2+}, Sr^{2+}, Ba^{2+})

Method 1. H_2L^{cat} (91.0 mg, 0.2 mmol) was added to pale-yellow mixtures of $(NEt_4)[AuCl_4]$ (46.9 mg, 0.1 mmol) and $M(NO_3)_2$ (0.05 mmol) (M = Ca^{2+}, Sr^{2+}, Ba^{2+}) in MeOH (2 mL) and a few drops of water were added. The ligand dissolved rapidly and the color of the solution changed from pale-yellow to colorless. The mixtures were stirred at room temperature for 30 min before 3 drops of Et_3N were added and the temperature was increased to 50 °C and kept for 1 h. The complexes deposited from the reaction mixtures as colorless solids, which were filtered off, washed with a small amount of MeOH and dried in vacuo.

Method 2. H_2L^{cat} (45.5 mg, 0.1 mmol) was added to mixtures of [Au(tht)Cl] (32.1 mg, 0.1 mmol) and $M(NO_3)_2$ (0.05 mmol) (M = Ca^{2+}, Sr^{2+}, Ba^{2+}) in MeOH (1.5 mL) and a few drops of water were added. The ligand dissolved rapidly and the mixtures were stirred at room temperature for 30 min. The addition of 2 drops of Et_3N caused the immediate deposition of the complexes of as colorless solids. After additional stirring for 1 h at 50 °C, the solids were filtered off, washed with a small amount of MeOH and dried in vacuo.

{Ca ⊂ $[Au_2(L^{cat}$-κ*S*$)_2]$} (1a): Yield: 40 % (27 mg) for method 1; 60 % (40 mg) for method 2. Elemental analysis calcd. for $C_{40}H_{56}N_8O_8S_4Au_2Ca$: C, 35.9; H, 4.2; N,8.4; S, 9.6 %; found C, 35.7; H, 4.4; N, 8.2; S, 9.3 %. IR (KBr, cm^{-1}): $\tilde{\nu}$ = 3364 (w), 2970 (w), 2928 (w), 1585 (s), 1503 (vs), 1427 (s), 1341 (s), 1238 (s), 1200 (s), 1119 (s), 1034 (s), 955 (m), 818 (m), 743 (m), 581 (m). ^1H NMR ($CDCl_3$, ppm): 7.01 (br, 8H, Ph); 4.90 (d, *J* = 13.5 Hz, 4H, OCH_2); 4.83 (d, *J* = 13.0 Hz, 4H, OCH_2); 3.64 (dq, *J* = 14.1 Hz, 7.1 Hz, 8H, NCH_2); 3.61 (dq, *J* = 14.1 Hz, 7.1 Hz, 4H, NCH_2); 3.25 (dq, *J* = 14.1 Hz, 7.1 Hz, 4H, NCH_2); 1.12 (t, *J* = 7.5 Hz, 12H, CH_3); 1.06 (t, *J* = 7.1 Hz, 12H, CH_3). $^{13}C\{^1H\}$ NMR ($CDCl_3$, ppm): 183.5 (C=O); 168.4 (C=S); 146.1, 121.8, 112.0 (Ph); 70.7 (OCH_2); 47.0, 46.2 (NCH_2); 12.7, 12.4 (CH_3). Single crystals for X-ray analysis were grown from CH_2Cl_2/MeOH.

{Sr ⊂ $[Au_2(L^{cat}$-κ*S*$)_2]$} (1b): Yield: 45 % (31 mg) for method 1; 67 % (46 mg) for method 2. Elemental analysis calcd. for $C_{40}H_{56}N_8O_8S_4Au_2Sr$: C, 34.6; H, 4.1; N,8.1; S, 9.3 %; found C, 34.8; H, 4.3; N, 7.9; S, 9.0 %. IR (KBr, cm^{-1}): $\tilde{\nu}$ = 2970 (w), 2928 (w), 1595 (s), 1503 (vs), 1429 (s), 1356 (s), 1238 (s), 1196 (s), 1117 (s), 1036 (s), 953 (m), 922 (m), 816 (m), 743 (m), 584 (m). ^1H NMR ($CDCl_3$, ppm): 7.09–7.04 (m, 8H, Ph); 4.95 (s, br, 8H, OCH_2); 3.72 (br, 8H, NCH_2); 3.48 (br, 8H, NCH_2); 1.24 (t, *J* = 7.0 Hz, 12H, CH_3); 1.11 (t, *J* = 7.0 Hz, 12H, CH_3). $^{13}C\{^1H\}$ NMR ($CDCl_3$, ppm): 182.4 (C=O); 168.9 (C=S); 146.2, 122.0, 112.3 (Ph); 71.2 (OCH_2); 47.0, 46.1 (NCH_2); 12.9, 12.5 (CH_3).

{Ba ⊂ $[Au_2(L^{cat}$-κ*S*$)_2]$} (1c): Yield: 43 % (31 mg) for method 1; 63 % (45 mg) for method 2. Elemental analysis calcd. for $C_{40}H_{56}N_8O_8S_4Au_2Ba$: C, 33.5; H, 3.9; N,7.8; S, 8.9 %; found C, 33.5; H, 4.0; N, 7.6; S, 8.8 %. IR (KBr, cm^{-1}): $\tilde{\nu}$ = 35024 (vw), 2974 (w), 2933 (w), 1570 (s), 1499 (vs), 1425 (s), 1344 (s), 1234 (vs), 1198 (s), 1119 (s), 1030 (s), 951 (m), 918 (m), 862 (m), 820 (m), 735 (m), 567 (m). ^1H NMR ($CDCl_3$, ppm): 7.04–6.99 (m, 8H, Ph); 4.94 (s, br, 8H, OCH_2); 3.76 (q, *J* = 7.5 Hz, 8H, NCH_2); 3.49 (q, *J* = 7.5 Hz, 8H, NCH_2); 1.31 (t, *J* = 7.0 Hz, 12H, CH_3); 1.10 (t, *J* = 7.0 Hz, 12H, CH_3). $^{13}C\{^1H\}$ NMR ($CDCl_3$, ppm): 183.3 (C=O); 168.4 (C=S); 146.6, 122.0, 112.7 (Ph); 71.8 (OCH_2); 47.2, 46.1 (NCH_2); 13.0, 12.6 (CH_3). Single crystals for X-ray analysis were grown from CH_2Cl_2/MeCN.

{2M ⊂ $[Au_4(L^{py}$-κ*S*$)_4]$} (M^{2+} = Ca^{2+}, Sr^{2+}, Ba^{2+})

The complexes were synthesized following method 2 described above. Single crystals suitable for X-ray diffraction were obtained from slow diffusion of MeOH into the solutions of complexes in CH_2Cl_2.

{2Ca ⊂ $[Au_4(L^{py}$-κ*S*$)]_4$} (2a): Yield: 48 % (62 mg). Elemental analysis: Calcd. for $C_{68}H_{102}O_{13}N_{20}S_8Au_4Ca_2$ ({2Ca ⊂ $[Au_4(L^{py})_4]$}·$5H_2O$): C, 32.3; H, 4.1; N, 11.1; S, 10.1 %; found C, 32.1; H, 4.1; N, 10.8; S, 10.1 %. IR (KBr, cm^{-1}): $\tilde{\nu}$ = 3431 (br, m), 2974 (m), 2931 (m), 2870 (w), 1602 (w), 1585 (w), 1554 (w), 1508 (s), 1458 (m) 1431 (m), 1406 (m), 1357 (s), 1315 (w), 1244 (s), 1201 (w), 1122 (s), 1076 (m), 1012 (w), 906 (w), 858 (w), 750 (m), 669 (w), 655 (w), 482 (w), 420 (w). ^1H NMR ($CDCl_3$, ppm): 7.98 (d, *J* = 7.5 Hz, 1H, Py); 7.92 (d, *J* = 7.5 Hz, 1H, Py); 7.73 (t, *J* = 7.5 Hz, 1H, Py); 3.76–3.28 (br, 8H, CH_2); 1.10 (t, *J* = 7.0 Hz, 6H, CH_3), 1.05 (t, *J* = 6.0 Hz, 6H, CH_3). $^{13}C\{^1H\}$ NMR ($CDCl_3$, ppm): 181.0, 179.7 (C=O); 168.0, 165.6 (C=S); 153.0, 152.4, 137.9, 125.9, 125.7 (Py); 46.6, 46.3, 45.9, 45.5 (CH_2); 12.7 (CH_3). ESI^+ MS (*m*/*z*): 2463.3379, 27 %, $[\{2Ca \subset [Au_4(L^{py})_4]\} + Na]^+$ (calcd. 2463.2984); 1850.2431, 9 %, $[\{2Ca \subset [Au_3(L^{py})_3]\}]^+$ (calcd. 1850.2128); 1259.1399, 30 %, $[\{Ca \subset [Au_2(L^{py})_2]\} + K]^+$ (calcd. 1259.1180); 1243.1665, 100 %, $[\{Ca \subset [Au_2(L^{py})_2]\} + Na]^+$ (calcd. 1243.1441).

{2Sr ⊂ $[Au_4(L^{py}$-κ*S*$)_4]$} (2b): Yield: 43 % (59.6 mg). Elemental analysis: Calcd. for $C_{68}H_{100}O_{12}N_{20}S_8Au_4Sr_2$ ({2Sr ⊂ $[Au_4(L^{py})_4]$}·$4H_2O$): C, 31.3; H, 3.9; N, 10.7; S, 9.8 %; found C, 31.5; H, 4.0; N, 10.3; S, 9.7 %. IR (KBr, cm^{-1}): $\tilde{\nu}$ = 3431 (br, m), 2974 (m), 2931 (m), 2870 (w), 1602 (w), 1583 (w), 1554 (m), 1508 (s), 1458 (s), 1431 (s), 1406 (s), 1356

(s), 1315 (w), 1244 (s), 1122 (m), 1076 (w), 1008 (w), 906 (w), 841 (w), 748 (m), 678 (w), 654 (w), 480 (w), 420 (w). ^{1}H NMR ($CDCl_3$, ppm): 7.98 (br, 2H, Py); 7.72 (t, J = 7.5 Hz, 1H, Py); 3.62–3.41 (br, 8H, CH_2); 1.09 (br, 12H, CH_3). ^{13}C{^{1}H} NMR ($CDCl_3$, ppm): 181.4 (C=O); 167.1 (C=S); 154.0, 137.7, 126.0 (Py); 46.4 (br, CH_2); 12.8 (CH_3). ESI$^+$ MS (*m/z*): 2537.2070, 14 % [{2Sr ⊂ [$Au_4(L^{py})_4$]} + H]$^+$ (calcd. 2537.2025); 1946.1044, 18 %, [{2Sr ⊂ [$Au_3(L^{py})_3$]}]$^+$ (calcd. 1946.0988); 1860.2139, 13 %, [{Sr ⊂ [$Au_3(L^{py})_3$]} + 2H]$^+$ (calcd. 1860.2089); 1291.0909, 17 %, [{Sr ⊂ [$Au_2(L^{py})_2$]} + Na]$^+$ (calcd. 1291.0871); 1269.1111, 21 %, [{Sr ⊂ [$Au_2(L^{py})_2$]} + H]$^+$ (calcd. 1269.1052); 1243.1478, 20 %, [{K ⊂ [$Au_2(L^{py})_2$]} + Na +H]$^+$ (calcd. 1243.1530); 1221.1660, 23 %, [{K ⊂ [$Au_2(L^{py})_2$]} + 2H]$^+$ (calcd. 1221.1711); 592.1146, 100 %, [{Au(L^{py})} + 2H]$^+$ (calcd. 592.1115).

{2Ba ⊂ [$Au_4(L^{py}$-κ*S*$)_4$]} (2c): Yield: 47 % (62 mg). Elemental analysis: Calcd. for $C_{68}H_{106}O_{15}N_{20}S_8Au_4Ba_2$ ({2Ba ⊂ [$Au_4(L^{py})_4$]}•$7H_2O$): C, 29.6; H, 3.9; N, 10.1; S, 9.3 %; found C, 29.3; H, 3.90; N, 9.9; S, 9.3 %. IR (KBr, cm^{-1}): $\tilde{\nu}$ = 3431 (br, m), 2974 (m), 2931 (m), 2870 (w), 1600 (w), 1550 (m), 1508 (s), 1431 (s), 1356 (s), 1315 (w), 1244 (s), 1120 (m), 1076 (m), 1005 (w), 906 (w), 841 (w), 746 (m), 680 (w), 653 (w), 480 (w), 420 (w). ^{1}H NMR ($CDCl_3$, ppm): 7.99 (br, 2H, Py); 7.69 (t, J = 7.5 Hz, 1H, Py); 3.62–3.47 (br, 8H, CH_2); 1.12 (br, 12H, CH_3). ^{13}C{^{1}H} NMR ($CDCl_3$, ppm): 178.8 (C=O); 168.7 (C=S); 154.4, 137.4, 126.3 (Py); 46.4, 45.8 (CH_2); 13.0, 12.9 (CH_3). ESI$^+$ MS (*m/z*): 2659.1751, 58 %, [{2Ba ⊂ [$Au_4(L^{py})_4$]} + Na]$^+$ (calcd. 2659.1837); 2046.0913, 12 %, [{2Ba ⊂ [$Au_3(L^{py})_3$]}]$^+$ (calcd. 2046.0981); 1341.0823, 86 % [{Ba ⊂ [$Au_2(L^{py})_2$]} + Na]$^+$ (calcd. 1341.0867); 1267.1070, 100 % [{Na ⊂ [$Au_2(L^{py})_2$]} + H_2O + 2Na]$^+$ (calcd. 1267.1716); 652.0231, 47 %, [{Au(L^{py})} + Na + K]$^+$ (calcd. 652.0493).

X-ray Crystallography. The intensities for the X-ray determinations of {Ca ⊂ [$Au_2(L^{cat}$-κ*S*$)_2$]} and {(MeCN)Ba ⊂ [$Au_2(L^{cat}$-κ*S*$)_2$]}•MeCN were collected on a Bruker D8 QUEST CMOS instrument at 100 K with Mo K_α radiation (λ = 0.71073 Å) using a TRIUMPH monochromator. The intensities for the X-ray determinations of {$(MeOH)_3(H_2O)Ca_2$ ⊂ [$Au_4(L^{py}$-κ*S*$)_4$]}•0.5CH_2Cl_2•2MeOH and {$(MeOH)_2(H_2O)_2Sr_2$ ⊂ [$Au_4(L^{py}$-κ*S*$)_4$]}•MeOH•1.5H_2O were collected on a Bruker D8 Venture instrument at 100 K with Mo K_α radiation (λ = 0.71073 Å) using a TRIUMPH monochromator, while the corresponding data for {(μ-H_2O)Ba_2 ⊂ [Au(L^{py}-κ*S*)]$_4$}•CH_2Cl_2•6MeOH were collected on a STOE IPDS 2T instrument at 200 K using Mo K_α radiation with a graphite monochromator. Standard procedures were applied for data reduction and absorption correction. Structure solutions and refinements were performed with the SHELXT and SHELXL 2014/7 programs included in the WinGX program package.[54–56] The structure of {$(MeOH)_2(H_2O)_2Sr_2$ ⊂ [$Au_4(L^{py}$-κ*S*$)_4$]}•MeOH•1.5H_2O was refined as a two-component twin. The final refinement was performed using HKLF 5 with reflection data prepared using TwinRotMat of PLATON program.[57] Hydrogen atoms were calculated for idealized positions and treated with the "riding model" option of SHELXL. More details on data collections and structure calculations are contained in Table 3. The representation of molecular structures was done using the program DIAMOND.[58] Since ball and stick presentations of the molecules are used in all of the Figures of this paper for reason of clarity, ellipsoid representations of all compounds are contained in the Supporting Information. Stereochemical analysis of the coordination spheres of the guest alkaline metal ions are performed by the program SHAPE 2.1.[59] More details about the analyses are contained in the Supporting Information.

Deposition Numbers 1950399, 1950400, 2021266, 2021267 and 2021268 contain the supplementary crystallographic data for this paper. These data are provided free of charge by the joint Cambridge Crystallographic Data Centre and Fachinformationszentrum Karlsruhe Access Structures service www.ccdc.cam.ac.uk/structures.

Acknowledgments

SFS is grateful for a "Science without Borders" fellowship of the Brazilian Council for Scientific and Technological Development (CNPQ), under project number 99999.009533/2013-03. CTP gratefully acknowledges financial support from the Vietnam National Foundation for Science and Technology Development (NAFOSTED) under grant number 104.03-2017.322. UA thanks the Dahlem Research School (DRS, FU Berlin) for financial support. We also gratefully acknowledge the assistance of the Core

Table 3. Crystal data and details of the structure determinations.

	{Ca ⊂ [$Au_2(L^{cat}$-κ*S*$)_2$]}	{(MeCN)Ba ⊂ [Au_2-(L^{cat}-κ*S*$)_2$]}•MeCN	{$(MeOH)_3(H_2O)Ca_2$ ⊂ [$Au_2(L^{py}$-κ*S*$)_2$]}•0.5CH_2Cl_2•2MeOH	{$(MeOH)_2(H_2O)_2Sr_2$ ⊂ [$Au_4(L^{py}$-κ*S*$)_4$]}•MeOH•1.5H_2O	{(μ-H_2O)Ba_2 ⊂ [$Au_4(L^{py}$-κ*S*$)_4$]}•CH_2Cl_2•6MeOH
Formula	$C_{40}H_{56}O_8N_8S_4Au_2Ca$	$C_{44}H_{62}O_8N_{10}S_4Au_2Ba$	$C_{73.5}H_{115}O_{14}N_{20}S_8ClAu_4Ca_2$	$C_{71}H_{109}O_{14.5}N_{20}S_8Au_4Sr_2$	$C_{75}H_{120}O_{15}N_{20}S_8Cl_2Au_4Ba_2$
Mw	1339.18	1518.55	2662.80	2694.36	2931.83
Crystal system	Monoclinic	Monoclinic	Monoclinic	Monoclinic	Monoclinic
a/Å	23.2665(9)	22.6724(16)	34.634(5)	35.077(3)	14.5416(6)
b/Å	14.7403(5)	12.7544(9)	14.6633(19)	14.6402(12)	14.3408(6)
c/Å	15.2530(5)	20.1143(16)	26.174(6)	26.3535(19)	27.3087(12)
α/°	90	90	90	90	90
β/°	111.742(1)	112.704(2)	128.923(3)	128.863(2)	102.291(4)
γ/°	90	90	90	90	90
V/Å^3	4859.0(3)	5365.8(7)	10341(3)	10537.9(14)	5564.4(4)
Space group	*C2/c*	$P2_1/c$	*Cc*	*Cc*	P2/n
Z	4	4	4	4	2
D_{calc}/g cm^{-3}	1.831	1.880	1.710	1.698	1.750
μ/mm^{-1}	6.366	6.394	6.006	6.772	6.208
No. reflect.	48563	54614	116408	277277	43038
No. indep.	6057	13230	23396	25243	9801
R_{int}	0.0485	0.0754	0.0279	0.0831	0.0849
No. param.	289	632	1102	922	619
R_1/wR_2	0.0219/0.0432	0.0413/0.0629	0.0251/0.0603	0.0420/0.0991	0.0544/0.1386
GOF	1.047	1.051	1.038	1.112	1.068
CCDC	1950399	1950400	2021266	2021267	2021268

Facility BioSupraMol supported by the DFG. Open access funding enabled and organized by Projekt DEAL.

Keywords: Gold(I) complexes · Aroylthioureas · Metallacoronates · Alkaline earth metals

[1] L. Beyer, E. Hoyer, H. Hennig, R. Kirmse, H. Hartmann, J. Liebscher, *J. Prakt. Chem.* **1975**, *317*, 829–839.
[2] G. Fitzl, L. Beyer, J. Sieler, R. Richter, J. Kaiser, E. Hoyer, *Z. Anorg. Allg. Chem.* **1977**, *433*, 237–241.
[3] L. Beyer, E. Hoyer, J. Liebscher, H. Hartmann, *Z. Chem.* **1981**, *21*, 81–91.
[4] R. Köhler, R. Kirmse, R. Richter, J. Sieler, E. Hoyer, L. Beyer, *Z. Anorg. Allg. Chem.* **1986**, *537*, 133–144.
[5] J. Sieler, R. Richter, E. Hoyer, L. Beyer, O. Lindqvist, L. Andersen, *Z. Anorg. Allg. Chem.* **1990**, *580*, 167–174.
[6] A. Mohamadou, I. Déchamps-Olivier, J.-P. Barbier, *Polyhedron* **1994**, *13*, 1363–1370.
[7] K. R. Koch, *Coord. Chem. Rev.* **2001**, *216–217*, 473–488.
[8] O. Hallale, S. A. Bourne, K. R. Koch, *CrystEngComm* **2005**, *7*, 161–166.
[9] A. Rodenstein, J. Griebel, R. Richter, R. Kirmse, *Z. Anorg. Allg. Chem.* **2008**, *634*, 867–874.
[10] H. H. Nguyen, C. T. Pham, A. Rodenstein, R. Kirmse, U. Abram, *Inorg. Chem.* **2011**, *50*, 590–596.
[11] N. Selvakumaran, N. S. P. Bhuvanesh, R. Karvembu, *Dalton Trans.* **2014**, *43*, 16395–16410.
[12] R. Richter, J. Sieler, R. Köhler, E. Hoyer, L. Beyer, L. K. Hansen, *Z. Anorg. Allg. Chem.* **1989**, *578*, 191–197.
[13] K. R. Koch, S. A. Bourne, A. Coetzee, J. Miller, *J. Chem. Soc., Dalton Trans.* **1999**, 3157–3161.
[14] K. R. Koch, O. Hallale, S. A. Bourne, J. Miller, J. Bacsa, *J. Mol. Struct.* **2001**, *561*, 185–196.
[15] S. A. Bourne, O. Hallale, K. R. Koch, *Cryst. Growth Des.* **2005**, *5*, 307–312.
[16] A. Rodenstein, R. Richter, R. Kirmse, *Z. Anorg. Allg. Chem.* **2007**, *633*, 1713–1717.
[17] A. N. Westra, S. A. Bourne, K. R. Koch, *Dalton Trans.* **2005**, 2916–2924.
[18] H. H. Nguyen, J. J. Jegathesh, A. Takiden, D. Hauenstein, C. T. Pham, C. D. Le, U. Abram, *Dalton Trans.* **2016**, *45*, 10771–10779.
[19] P. Chien Thang, N. Hung Huy, A. Hagenbach, U. Abram, *Inorg. Chem.* **2017**, *56*, 11406–11416.
[20] P. C. Thang, N. H. Huy, U. Abram, *Eur. J. Inorg. Chem.* **2018**, *2018*, 951–957.
[21] C. D. Le, C. T. Pham, H. H. Nguyen, *Polyhedron* **2019**, *173*, 114143.
[22] C. T. Pham, T. H. Nguyen, K. Matsumoto, H. H. Nguyen, *Eur. J. Inorg. Chem.* **2019**, *2019*, 4142–4146.
[23] C. T. Pham, T. H. Nguyen, T. N. Trieu, K. Matsumoto, H. H. Nguyen, *Z. Anorg. Allg. Chem.* **2019**, *645*, 1072–1078.
[24] Y.-M. Zhang, H.-X. Pang, C. Cao, T.-B. Wei, *J. Coord. Chem.* **2008**, *61*, 1663–1670.
[25] N. Gunasekaran, P. Ramesh, M. N. G. Ponnuswamy, R. Karvembu, *Dalton Trans.* **2011**, *40*, 12519–12526.
[26] N. Gunasekaran, S. W. Ng, E. R. T. Tiekink, R. Karvembu, *Polyhedron* **2012**, *34*, 41–45.
[27] N. Selvakumaran, L. Sandhiya, N. S. P. Bhuvanesh, K. Senthilkumar, R. Karvembu, *New J. Chem.* **2016**, *40*, 5401–5413.
[28] U. Braun, R. Richter, J. Sieler, A. I. Yanovsky, Y. T. Struchkov, *Z. Anorg. Allg. Chem.* **1985**, *529*, 201–208.
[29] R. Richter, F. Dietze, S. Schmidt, E. Hoyer, W. Poll, D. Mootz, *Z. Anorg. Allg. Chem.* **1997**, *623*, 135–140.
[30] U. Schröder, L. Beyer, J. Sieler, *Inorg. Chem. Commun.* **2000**, *3*, 630–633.
[31] H. G. Berhe, S. A. Bourne, M. W. Bredenkamp, C. Esterhuysen, M. M. Habtu, K. R. Koch, R. C. Luckay, *Inorg. Chem. Commun.* **2006**, *9*, 99–102.
[32] M. M. Habtu, S. A. Bourne, K. R. Koch, R. C. Luckay, *New J. Chem.* **2006**, *30*, 1155–1162.
[33] R. Richter, J. Sieler, L. Beyer, O. Lindqvist, L. Andersen, *Z. Anorg. Allg. Chem.* **1985**, *522*, 171–183.
[34] R. Richter, J. Sieler, R. Köhler, E. Hoyer, L. Beyer, I. Leban, L. Golič, *Z. Anorg. Allg. Chem.* **1989**, *578*, 198–204.
[35] Z. Weiqun, Y. Wen, Q. Lihua, Z. Yong, Y. Zhengfeng, *J. Mol. Struct.* **2005**, *749*, 89–95.
[36] W. Bensch, M. Schuster, *Z. Anorg. Allg. Chem.* **1992**, *611*, 99–102.
[37] V. D. Schwade, L. Kirsten, A. Hagenbach, E. S. Lang, U. Abram, *Polyhedron* **2013**, *55*, 155–161.
[38] O. E. Piro, E. E. Castellano, R. C. V. Piatti, A. E. Bolzan, A. K. Arvia, *Acta Crystallogr., Sect. C* **2002**, *58*, m252–m255.
[39] S. Friedrichs, P. G. Jones, *Acta Crystalogr.* **1999**, *C55*, 1625–1627.
[40] M. S. Hussain, A. A. Isab, *Trans. Met. Chem.* **1985**, *10*, 178–181.
[41] S. Friedrichs, P. G. Jones, *Z. Naturforsch. B* **2004**, *59*, 49–57.
[42] M. Fettouhi, A. A. Isab, M. I. M. Wazeer, *Z. Kristallogr. New Cryst. Struct.* **2004**, *219*, 391–392.
[43] M. B. Cingi, F. Bigoli, M. Lanfranchi, E. Leporati, M. A. Pellinghelli, C. Foglia, *Inorg. Chim. Acta* **1995**, *235*, 37–43.
[44] A. A. A. Suleiman, N. Kalia, G. Bhatia, M. Kaur, M. Fettouhi, M. Altaf, N. Baig, A.-N. Kawde, A. A. Isab, *New J. Chem.* **2019**, *43*, 14565–14574.
[45] A. C. Fabretti, A. Giusti, W. Malavasi, *J. Chem. Soc. Dalton Trans.* **1990**, 3091–3093.
[46] L. C. Porter, J. P. Fackler Jr., J. Costamagna, R. Schmidt, *Acta Crystallogr., Sect. C* **1992**, *48*, 1751–1754.
[47] S. Friedrichs, P. G. Jones, *Z. Naturforsch. B* **2004**, *59*, 793–801.
[48] W. Bensch, M. Schuster, *Z. Anorg. Allg. Chem.* **1992**, *611*, 95–98.
[49] D. Casanova, M. Llunell, P. Alemany, S. Alvarez, *Chem. Eur. J.* **2005**, *11*, 1479–1494.
[50] A. Ruiz-Martínez, D. Casanova, S. Alvarez, *Chem. Eur. J.* **2008**, *14*, 1291–1303.
[51] A. Ruiz-Martínez, D. Casanova, S. Alvarez, *Dalton Trans.* **2008**, 2583–2591.
[52] H. Huy Nguyen, V. M. Deflon, U. Abram, *Eur. J. Inorg. Chem.* **2009**, *2009*, 3179–3187.
[53] R. Uson, A. Laguna, M. Laguna, D. A. Briggs, H. H. Murray, J. P. Fackler, *Inorg. Synth.* (Ed.: H. D. Kaesz), **2007**, pp. 85–91.
[54] G. Sheldrick, *Acta Crystallogr., Sect. A* **2015**, *71*, 3–8.
[55] G. Sheldrick, *Acta Crystallogr., Sect. C* **2015**, *71*, 3–8.
[56] L. Farrugia, *J. Appl. Crystallogr.* **2012**, *45*, 849–854.
[57] A. Spek, *Acta Crystallogr., Sect. D* **2009**, *65*, 148–155.
[58] *DIAMOND*, vers. 4.5.2, Crystal Impact - Dr. H. Putz & Dr. K. Brandenburg GbR, Kreuzherrenstr. 102, 53227 Bonn, Germany, **2018**.
[59] S. Alvarez, P. Alemany, D. Casanova, J. Cirera, M. Llunell, D. Avnir, *Coord. Chem. Rev.* **2005**, *249*, 1693–1708.

Received: August 12, 2020